Integrating Model Based and Data Driven Approaches for the Automatic Segmentation of Cardiac Short-Axis Cine MRI Recordings

A Müller[1], A Neitmann[2], M Kunze[3], N Merkle[3], M Höher[4]
V Hombach[3], J Wöhrle[3], H Neumann[2], HA Kestler[1,2,3]

[1]University Hospital Ulm, Internal Medicine I, Ulm, Germany
[2]University of Ulm, Neural Information Processing, Ulm, Germany
[3]University Hospital Ulm, Internal Medicine II, Ulm, Germany
[4]Klinikum Bayreuth, Germany

Abstract

A robust model-based segmentation method for automatically detecting left ventricular endocardial borders in cardiac MRI short-axis slices is proposed. The method is evaluated with expert drawn contours on an extended dataset (83 cases).

The contour detection involves the four steps: (a) A region of interest enclosing the left ventricle is computed using a size invariant circular Hough transform. (b) Segmentation is performed by an adaptive threshold detection method taking model-based information into account. (c) Papillary muscles are included into the endocardial border by merging scattered regions and interpolating the resulting contour with approximating periodic splines. (d) Outliers and partially wrong contours are finally removed by applying a three dimensional median filter.

1. Introduction

In patients with reduced left ventricular function (LVF) the frequently concomitant left bundle branch block (LBBB) leads to a further deterioration of global heart performance due to asynchronous contraction. Implantation of biventricular pacemakers may be an option for these patients [2]. QRS duration alone has failed to serve as predictive parameter for the clinical outcome of patients after biventricular pacing, since ventricular synchronicity does not necessarily require a synchronous electrical excitation [3]. In previous studies [1, 4, 5] we showed the utility of measuring phase differences in left ventricular contours.

As a major part in finding these phase differences is the detection of the left ventricular endocardial borders we focused this study on finding these contours automatically.

2. Methods

2.1. Subject data

The subject group of a previous study [1] was extended to 65 subjects with dilated cardiomyopathy (DCM) from which 35 had a left bundle branch block (LBBB), and 20 healthy subjects. Due to low image quality and non-uniform brightness distribution two MR recordings had to be excluded: one from the LBBB group and one from the DCM w/o LBBB group.

The remaining 63 DCM patients had an average left ventricular ejection fraction (LVEF) of 26.7% with standard deviation 9.2%. The control group had an average LVEF of 70.3% with standard deviation 4.8%.

2.2. Imaging

Imaging was performed on a $1.5T$ whole body scanner (Intera CV, Philips Medical Systems, Software Release 9.1) with Master Gradients (slew rate $150T/m/s$, amplitude $30mT/m$). A 5-element phased-array cardiac coil was used. Three short survey scans were performed to define position and true axis of the left ventricle. Afterwards, wall motion was imaged during breath holding within long and short-axis slices using a steady-state free precession (balanced fast-field echo) sequence, which provided an excellent endocardial contrast. Cardiac synchronization was achieved by prospective gating. The cine images were recorded with 23 or 32 frames per heart beat and with a slice thickness of $10mm$ ($8mm$ in some cases).

2.3. Image analysis

All endocardial borders of the left ventricle were manually drawn by an expert (five inner short axis slices) for

the whole cardiac cycle using the MASS® plus 5.0 Software (Medis, Leiden, Netherlands). Difficulties in the correct tissue assignment were reduced by observing adjacent slices and time frames in the detection process. The papillary muscles were assigned to the ventricular cavum. Further data processing was performed with Matlab® 7.04 (MathWorks Inc.).

2.4. Automatic contour detection

The gray valued MR images were streched to the interval $[0, 1]$. The resolution of the MR images was reduced by sub-sampling to 400×400 pixels for faster image processing.

2.4.1. Region of Interest Selection

In a first step a rectangular region of interest (ROI) enclosing the left ventricle is detected [1]to obtain a point $\mathbf{p}_0$ in the endocardium by the use of a circular Hough transform [6, 7, 8]. For this step a pre-segmentation was performed with Otsus thresholding method [9]. The ROI is computed for the first time frame $t = 1$ of each slice and is used for all other time frames $t > 1$. This seems a reasonable choice as the first time frame corresponded to the heart in its relaxed state before contraction.

For each time-frame $t = 1 \ldots T$ the following procedure is repeated and leads to a first estimate of the left ventricular endocardial pixel sets which is then used to determine the center point $\mathbf{p}_t$ of the main region.

1. Clip the image to the ROI.
2. Segment the image with Otsus method (threshold θ_g).
3. Apply morphological opening (circular shape, radius 20 pixel) to remove noisy structures.
4. Select the region which covers the point $\mathbf{p}_{t-1}$ and compute its center of gravity $\mathbf{p}_t$.

2.5. Threshold Optimization

For the final segmentation of the ROI a global threshold value $\theta^* \in [0, 1]$ is optimized for each image. As contrast and brightness of the MR images vary over time frames an adaptive threshold detection method is employed integrating model based information such as contrast and brightness in the vicinity of the found contour, the circular shape of the left ventricle, and a predicted contour estimated from previous time frames.

For different threshold values in the range $[\theta_1, \theta_2]$ the ROI is segmented and the resulting contour is computed. Each θ is evaluated by the error functional $E(\theta)$. The threshold θ^* for which E is minimal is used for the segmentation yielding the final contour $c_{s,t}$ for slice s and time frame t. For the first time frame $t = 1$ the search range $[\theta_g - 40/256, \theta_g + 20/256]$ was determined by a window around the threshold θ_g found by Otsus method [9]. Twenty equally sampled values were generated. For the time frames $t > 1$ the threshold range was set to $[\theta^*_{(t-1)} - 20/256, \theta^*_{(t-1)} + 20/256]$ and 10 values were sampled.

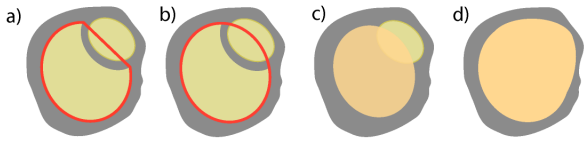

Figure 1. Region Selection: (a) The convex hull of the main region is determined. (b) Weighted interpolation of the convex hull by a periodic spline. (c) Find intersecting regions in the surrounding area. (d) Extension of the contour by merging with intersecting regions and a further convex hull and spline interpolation step. Papillary muscles near the ventricular border lead to cut off contours and even sometimes to topologically disconnected regions in the segmented image. In those cases the convex hull of the main region has long line segments clipping parts of the ventricle. The above method tries to merge isolated regions in order to complete the endocardial contour. The pre-information that the left ventricle is circular shaped was reflected by using cubic periodic approximating splines.

The following steps are executed for each threshold θ to acquire the contour $c^{(\theta)}$:

1. Clip the image to the ROI.
2. Segment the image with the threshold θ.
3. Trace the boundary of the main left ventricular region by selecting the connected region $\mathbf{R}_t$ which covers the point $\mathbf{p}_t$.
4. Compute the convex hull of the main region.
5. Interpolate the convex hull with a periodic smoothing cubic 1-d spline (see below).
6. Merge the main region with all connected regions (4 neighborhood) which intersect the spline-contour and have less than 5% of the pixels of the main region (see Figure 1.
7. Repeat the steps 4. and 5. for the new compound region to achieve the final contour $c^{(\theta)}$.
8. Sample the contour at $n = 128$ equiangular steps to the center of the contour.

For the time frames $t > 2$ a predicted contour c^*_t is estimated by linearly extrapolating the contours of the last two time steps. Hereto the two contours c_{t-2} and c_{t-1} are sampled at 128 equiangular points relative to the center of c_{t-2}. The radii of the interpolated contour were estimated as $r^*_i(t) = 2 \cdot r^*_i(t-1) - r^*_i(t-2)$. The distance $d(c^*, c^{(\theta)})$ of the contour $c^{(\theta)}$) obtained by the threshold value θ to the predicted contour c^* was defined as $1/n \sum_i |r^*_i - r^{(\theta)}_i|$.

Error Functional

The error functional $E(\theta)$ requires the computation of two further contours: The outer contour $c_o^{(\theta)}$ is acquired by extending $c^{(\theta)}$ radially to its center by $\Delta = ROI_y/60$ pixels; a 60th of the height of the ROI. An inner contour $c_i^{(\theta)}$ is determined by morphological erosion of the main region $\mathbf{R}_t$ with a circular shaped structural element with diameter Δ and a tracing of the boundary of this region (see Figure 2).

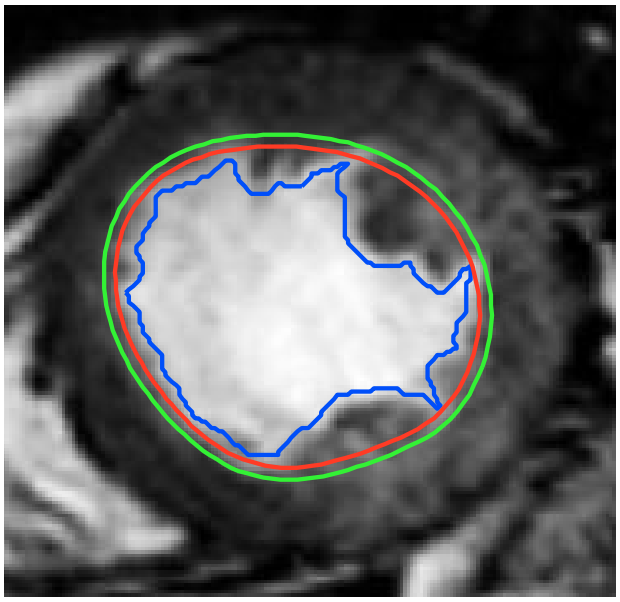

Figure 2. The inner $c_i^{(\theta)}$ (blue), outer $c_o^{(\theta)}$ (green), and actual contour $c^{(\theta)}$ (red) are shown for the ROI of a short-axis slice. If the threshold θ reaches an acceptable value the mean brightness of the inner contour m_i becomes high and those of the outer contour m_o - lying in the wall - becomes low. The variances s_i and s_o should become low in this case.

The proposed error functional $E(\theta)$ consists of the following parts:

- The mean brightness of the inner (bright) I_i and outer (dark) I_o pixels as determined by Otsus threshold.
- The intensity values along the outer contour $x_o(k), k = 1 \dots n_o$ and the inner contour $x_i(k), k = 1 \dots n_i$.
- Mean and standard deviation of the intensity values along the outer contour m_o and s_o and the inner contour m_i and s_i.
- Square distances of the intensity values of the inner contour to the mean brightness I_i which are too dark: $f_i = 1/n_i \sum_{k=1}^{n_i} H_+(I_i - x_i(k))^2$ for the threshold function $H_+(x)$ which is x for $x > 0$ and 0 otherwise.
- Square distances of the intensity values of the outer contour to the mean brightness I_o which are too bright: $f_o = 1/n_o \sum_{k=1}^{n_o} H_+(x_o(k) - I_o)^2$.
- The relative mean difference d_{mean} to the predicted contour: $d(c^*, c^{(\theta)})/\bar{r}$ for the mean radius $\bar{r}$ of $c^{(\theta)}$.
- The difference of the maximum radius distance between the contours c^* and $c^{(\theta)}$ relative to $\bar{r}$: d_{max}.

The error functional

$$E(\theta) = 20 \cdot \left[(f_o + \frac{f_i}{6}) + \frac{1}{4}(s_o + \frac{s_i}{6}) + \frac{1}{6}(m_o - \frac{m_i}{6}) \right] + 2 \cdot d_{max} + d_{mean}$$

reflects the model assumptions: 1) the variance should be low in the inner and outer contours, 2) the difference of the mean brightnesses of the inner and outer contour should be high, 3) the found contour should be in the nearness of the predicted contour c^*.

2.5.1. Spline Interpolation

Papillary muscles lying at the endocardial wall often obscure the ventricular contour. Hereto an approximating weighted periodic cubic smoothing spline [10],[11, Chapter 5] is used to interpolate missing parts of the contour that are detected by finding regions where the convex hull does not cover the endocardial main small environment. To determine these regions the spline curve is sampled at $n = 128$ equiangular steps and the binary image was dilated by a circular structural element of size 5×5. As the approximation is applied to the radius profile relative to the center of gravity a one-dimensional spline was sufficient. The smoothing factor is set to twice the number of gap pixels $0 \leq n_g \leq n$ but at least to 40. For the contour a binary vector $\mathbf{b} \in \{0,1\}^n$ is constructed which contains a 1 for each present point (covering the main region) and a 0 for each gap point. A circular morphological closing on $\mathbf{b}$ with window size 11 removes small gap regions and a subsequent circular erosion with window size 5 smoothes the edges into the gap regions resulting in the new binary vector $\hat{\mathbf{b}}$. The number of gaps is $n_g = \#\{k \mid b_k = 0\}$ and the spline weights were set to $w(k) = 0.1$ for all $b_k = 0$ (gap) and $w(k) = 0.8$ for all $b_k = 1$ (present) such that the missing contour parts are smoothed stronger by lower weights.

2.5.2. Continuity correction

Discontinuities and outliers of the contour motions were enhanced by using a median filter of window size $w = 3$ over adjacent time frames and slices. For each slice s the mean center $\bar{\mathbf{m}}_s$ over all time frames is computed and all contours $c_{s,t}$ were resampled relative to $\bar{\mathbf{m}}_s$ at the angles $\theta_k = 2\pi\frac{k}{n}$, $k = 0 \dots n-1$ for $n = 128$ yielding radius profiles $r_{s,t}(k) > 0$. The different diameters of the slices were adapted before filtering for s and

$s' = s-w \dots s+w$ by $\hat{r}^{(s)}_{s',t}(k) = r_{s,t}(k) \cdot u_s(k)/u_{s'}(k)$, $k = 1 \dots n$ with the median radii over all phases being $u_s(k) = \text{median}\{r_{s,t}(k) \mid k = 1 \dots n\}$. The filtered signals became $r'_{s,t} = \text{median}\{\hat{r}^{(s)}_{s',t'} \mid s-w \leq s' \leq s+w, t-w \leq t' \leq t+w\}$ and were then transformed back into cartesian coordinates yielding the final post-processed contours $\hat{c}_{s,t}$.

Outliers, where the contour of a single time frame was erroneous (e.g. due to bad segmentation, the endocardial region became spuriously connected to a region outside the endocardium), could be removed successfully with this method.

3. Results

The following three contours were compared:
A: The convex hull of the connected main region of the left ventricle segmented by the optimized threshold θ^* .
B: The spline-interpolated contours $c_{s,t}$ before median filtering.
C: The median filtered contours $\hat{c}_{s,t}$.
by measuring the deviation to the manually drawn contours. The mean absolute radius deviations (sampled over $n = 128$ equiangular steps) were A: 3.50 ± 1.95, B: 3.09 ± 1.89, and C: 2.99 ± 1.67. These values represent pixels in the scaled 400×400 image. The three contour detection methods were compared using a paired Wilcoxon rank sum test. Method B had lower deviations than A and C a lower deviation than B (p-values $< 2.2e-16$).

4. Discussion and conclusions

A fast method for automatically tracing the left ventricular endocardial border in cardiac MRI was proposed. Preknowledge was included by constructing an error function that incorporates prior experience segmenting the endocardial border of the left ventricle on these images. Furthermore adjacent time frames and slices were used to stabilize the found contours and remove artifacts. The usefulness of the spline interpolation in combination with the median filtering was shown by comparing these to manually drawn contours.

Acknowledgements

AM and AN contributed equally to this work and should both be considered first authors. HN and HAK should both be considered senior authors. We would like to thank Günther Palm, Neuroinformatics, University of Ulm and Thorsten Nusser and Katja Hertner from the Department of Internal Medicine II, Cardiology, University Hospital of Ulm for fruitful discussions. This work was supported in part by grants from the "Stifterverband für die Deutsche Wissenschaft" (HAK) and the "Deutsche Forschungsgemeinschaft" (HAK and AM).

References

[1] Müller A, Neitmann A, Merkle N, Woehrle J, Hombach V, Kestler HA. Contour Detection of Short Axis Slice MR Images for Contraction Irregularity Assessment. In Computers in Cardiology, volume 32. IEEE, 2005; 21–24.

[2] Cazeau S, Leclercq C, Lavergne T, Walker S, Varma C, Linde C, Garrigue S, Kappenberger L, Haywood GA, Santini M, Bailleul C, Daubert JC. Effects of multisite biventricular pacing in patients with heart failure and intraventricular conduction delay. N Engl J Med 2001;344(12):873–880.

[3] Leclercq C, Faris O, Tunin R, Johnson J, Kato R, Evans F, Spinelli J, Halperin H, McVeigh E, Kass DA. Systolic improvement and mechanical resynchronization does not require electrical synchrony in the dilated failing heart with left bundle-branch block. Circ 2002;106(14):1760–1763.

[4] Müller A, Merkle N, Hombach V, Grebe O, Nusser T, Wöhrle J, Binner L, Kestler HA. Extracting robust features from cardiac magnetic resonance image contours for detecting dilated cardiomyopathy. In Computers in Cardiology, volume 31. IEEE, 2004; 157–160.

[5] Grebe O, Müller A, Merkle N, Wöhrle J, Binner L, Höher M, Hombach V, Neumann H, Kestler HA. Estimation of intra- and inter-ventricular dyssynchronization with cardiac magnetic resonance imaging. In Computers in Cardiology, volume 30. IEEE, 2003; 741–743.

[6] Kimme C, Ballard D, Sklansky J. Finding circles by an array of accumulators. Commun ACM 1975;18(2):120–122.

[7] Atherton TJ, Kerbyson DJ. Size invariant circle detection. Image Vision Comput 1999;17(11):795–803.

[8] Kälviäinen H, Hirvonen P, Xu L, Oja E. Probabilistic and non-probabilistic hough transforms: overview and comparisons. Image and Vision Computing 1995;13(4):239–252.

[9] Otsu N. A threshold selection method from gray-level histograms. IEEE Transactions on Systems Man and Cybernetics 1979;9(1):62–66.

[10] Dierckx P. Algorithms for smoothing data with periodic and parametric splines. Computer Graphics and Image Processing 1982;20:171–184.

[11] Dierckx P. Curve and surface fitting with splines. Monographs on numerical analysis Oxford science publications. Oxford University Press, 1995. ISBN 0-19-853441-8, 0-19-853440-X.

Address for correspondence:

Hans A. Kestler
University of Ulm
Internal Medicine I / Bioinformatics
Robert-Koch-Str. 8
89081 Ulm, Germany
hans.kestler@uni-ulm.de